Eurographics Conference on Visualization (EuroVis) 2015
H. Carr, K.-L. Ma, and G. Santucci
(Guest Editors)

Volume 34 (2015), Number 3

Supplemental Materials of Evaluating 2D Flow Visualization Using Eye Tracking

Hsin-Yang Ho[1], I-Cheng Yeh[2], Yu-Chi Lai[3], Wen-Chieh Lin[1], and Fu-Yin Cherng[1]

[1]National Chiao Tung University, Hsinchu, Taiwan
[2]Innovation Center for Big Data and Digital Convergence, Yuan Ze University, Chung-Li, Taiwan
[3]National Taiwan University of Science and Technology, Taipei, Taiwan

1. Background

We describe the background related to this study, including vector fields and eye tracking analysis.

Eye tracking analysis. When watch 2D images, the scan path of our eyes is not a smooth curve but a series of short stops and quick movements over the interesting regions. The short stops are called *fixations* and the fast movement between two fixations is called *saccade*. According to [Yar], an observer's scan paths may be totally different when performing different visual tasks, even though the observed image is the same. Jacob et al. [JK03] show that the fixation statistics, including the number of fixations, the averaging time of each fixation, and the average length of consecutive fixations, can be used to analyze the performance of our concentration during the viewing process.

Vector Fields. A vector field $\mathbf{v}$ can be described by the following equation [PPF*11]:

$$\dot{\mathbf{x}}(t) = \mathbf{v}(\mathbf{x}(t), t), \tag{1}$$

If a vector field $\mathbf{v}$ does not vary with time t, the field is called steady/autonomous/time-independent; Otherwise, the field is called unsteady/non-autonomous/time-dependent. Generally, the structures of a vector field, such as *streamlines*, *pathlines*, and *streaklines*, can be expressed as a set of curves. A streamline is a curve whose tangent at a location is parallel to the direction of the field at that location at a specific time instant. A pathline represents the trajectory of a particle moving along the field with time after releasing at a location in the field; A streakline is the locus of points of all the particles that have passed continuously through a particular location in the past. Intuitively, streamlines represent the state of a vector field at a specific time instant, while pathlines and streaklines represent the change of the field along the time. For a steady vector field, its streamlines, pathlines, and streaklines are the same.

A location in a vector field where the velocity (magnitude) is zero is called a critical point or stationary point. In 2D vector fields, there exist only certain types of critical points. Let $\dot{\mathbf{x}} = \mathbf{A}\mathbf{x}$ be the 2D linear system formed at a first-order critical point. According to the eigenvalues of $\mathbf{A}$, the critical point can be classified into six types as listed in Table 1. For the classification of higher-order singularities, please refer to the book by Firby and Gardiner [FG01].

Table 1: *Six types of critical points.*

$\mathbf{A} \in \mathbb{R}^{2\times 2}$ has two eigenvalues $a_1 + b_1 i$ and $a_2 + b_2 i$.				
saddle:	$a_1 a_2 < 0$,		$b_1 = b_2 = 0$.	
node sink:	$a_1 < 0$,	$a_2 < 0$,	$b_1 = b_2 = 0$.	
node source:	$a_1 > 0$,	$a_2 > 0$,	$b_1 = b_2 = 0$.	
focus sink:	$a_1 < 0$,	$a_2 < 0$,	$b_1 \neq 0$,	$b_2 \neq 0$.
focus source:	$a_1 > 0$,	$a_2 > 0$,	$b_1 \neq 0$,	$b_2 \neq 0$.
center:	$a_1 = a_2 = 0$,		$b_1 \neq 0$,	$b_2 \neq 0$.

2. Vector Field design method

Zhang et al. [ZMT06] proposed a vector field design approach to generate customized vector fields by summing several basis vector fields. A basis vector field contains only one critical point defined at the central location and controlled by a set of control factors. It is generated using van Wijk's basis vector approach [vW02]. For a field containing a critical point at a location $\mathbf{p}_0 = [x_0, y_0]^T$, the field at an arbitrary position $\mathbf{p} = [x, y]^T$ can be expressed as follow:

$$\mathbf{v}(\mathbf{p}) = ce^{-d\|\mathbf{p}-\mathbf{p}_0\|^2}\mathbf{M}(\mathbf{p}-\mathbf{p}_0), \tag{2}$$

where c is a scaling constant, d is a distance decay constant, and $\mathbf{M}$ is a 2×2 matrix. As discussed in Section 1, $\mathbf{M}$ has two eigenvalues: $\lambda_1 = a_1 + b_1 i$ and $\lambda_2 = a_2 + b_2 i$. We can adjust the eigenvalues and eigenvectors of $\mathbf{M}$ to control the magnitude and direction of a vector field.

In this paper, we set both eigenvalues to be real numbers

($b_1 = b_2 = 0$) because it is hard to control the magnitude of the field intuitively if either eigenvalue is a complex number. Under this condition, the magnitude of the field can be controlled by the eigenvalues easily, but only saddle, node sink, or node source can be generated. To generate focus sink and focus source, we use multiple vector fields of node sink, node source, or center to compose them. According to Helmholtz's theorem, a basis field with a focus sink can be decomposed into a field with a node sink and a field with a center; a field with a focus source can be decomposed into a field with a node source and a field with a center. To achieve these decomposition purposes, the field at an arbitrary position $\mathbf{p} = [x, y]^T$ is expressed as:

$$\mathbf{v}(\mathbf{p}) = c_{i_1} e^{-d_{i_1}\|\mathbf{p}-\mathbf{p}_i\|^2} \mathbf{M}_{i_1}(\mathbf{p}-\mathbf{p}_i) + c_{i_2} e^{-d_{i_2}\|\mathbf{p}-\mathbf{p}_i\|^2} \mathbf{M}_{i_2}(\mathbf{p}-\mathbf{p}_i), \tag{3}$$

where c_{i_1} and c_{i_2} are the control factors for the two fields with different types of critical points. As our experiments do not have any tasks of identifying a center, the center-type critical point is only needed for composing other types of critical points. Therefore, we generate a center-type vector field using a fixed setting: $\mathbf{M}_{i_2} = \begin{pmatrix} 0 & -1 \\ 1 & 0 \end{pmatrix}$ or $\begin{pmatrix} 0 & 1 \\ -1 & 0 \end{pmatrix}$. We can then adjust the real-valued eigenvalues and eigenvectors of $\mathbf{M}_{i_1}$, c_{i_1} and c_{i_2} to generate a basis vector field with a specific type of critical point. The fields used in the experiments are then constructed by weightedly summing several basis vector fields, each of which has a distinct type of critical point.

3. Mathematically Synthesized Flow Fields

All the flow fields used in this paper have the resolution of 800×800 pixels. We generate two types of fields: (1) random placement and (2) fixed placement of critical points. The first type is generated by randomly placing three to seven critical points of various types inside a square of 560×560 pixels located at the center as shown in Figure 1. For each basis field, we randomly set the value of c_{i_2} (see Section 2). If $c_{i_2} = 0$, the first set of parameters in Table 3 is used to generate the basis vector field; otherwise, the second set is used. The angle between the x-axis and the first eigenvector is set as $r(0, 2\pi)$, and the angle between the first and second eigenvectors is set as $\pm r(\frac{\pi}{3}, \frac{2\pi}{3})$, where $r(a,b)$ denotes a random number sampled from a uniform distribution $U(a,b)$. We control the flow speed (magnitude) in all vector fields at a similar range with a maximum of 400 pixel/sec and nonlinearly scale the flow speed such that 90% of samples have its speed greater than 40% of the maximal speed.

The second type of flow fields is generated by placing five critical points on the vertices of a pentagon located in the center of the image. The distance from the center of the pentagon to each vertex is 200 pixels. The parameters of these critical points are listed in Table 3. A larger decay constant is chosen so that the interference between adjacent critical points is minimized. We control the flow speed in all vector fields at a similar range with a maximum of 400 pixel/sec and nonlinearly scale the flow speed such that 80% of samples have its speed greater than 10% of the maximal speed. Figure 2 shows several examples of the second type of flow fields.

Table 2: *Parameters used in the first type of mathematically synthesized vector fields: random placement of critical points. $r(A,B)$ is a random number sampled from $U(A,B)$*

	1st *set*	2nd *set*
c_{i_1}	$r(0.8, 1.2)$	$r(0.8, 1.2)$
d_{i_1}	$r(0.036, 0.044)$	$r(0.036, 0.044)$
c_{i_2}	0	$r(1.2, 1.8)$
d_{i_2}		$r(0.036, 0.044)$
$\mathbf{M}_{i_1}$'s λ_1	$\pm r(0.8, 1.2)$	$\pm r(0.8, 1.2)$
$\mathbf{M}_{i_1}$'s λ_2	$\pm r(0.8, 1.2)$	$\pm r(0.8, 1.2)$

Table 3: *Parameters for the second type of mathematically synthesized vector fields: fixed placement of critical points.*

	saddle	node sink	node source	focus sink	focus source
c_{i_1}	$r(0.8, 1.2)$	$r(0.8, 1.2)$	$r(0.8, 1.2)$	$r(0.3, 0.4)$	$r(0.3, 0.4)$
d_{i_1}	0.2	0.2	0.2	0.2	0.2
c_{i_2}	0	0	0	$r(0.6, 0.8)$	$r(0.6, 0.8)$
d_{i_2}				0.2	0.2
$\mathbf{M}_{i_1}$'s λ_1	$r(0.8, 1.2)$	$r(0.8, 1.2)$	$r(-1.2, -0.8)$	$r(0.8, 1.2)$	$r(-1.2, -0.8)$
$\mathbf{M}_{i_1}$'s λ_2	$r(-1.2, -0.8)$	$r(0.8, 1.2)$	$r(-1.2, -0.8)$	$r(0.8, 1.2)$	$r(-1.2, -0.8)$

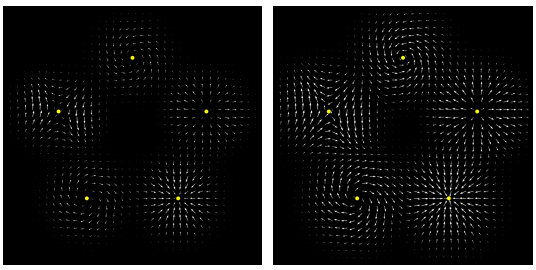

(a) (b)

Figure 2: *The second type of mathematically synthesized vector fields: fixed placement of critical points. (a) a vector field with five critical points. (b) adjusting the speed of the vector field.*

4. Boundary Conditions of Physical Simulation

The goal of our physical simulation is to generate complex flow patterns containing vortices. With the help of fluid simulation experts, we set the boundary conditions as shown in Figure 3 in order to create vortices.

© 2015 The Author(s)
Computer Graphics Forum © 2015 The Eurographics Association and John Wiley & Sons Ltd.

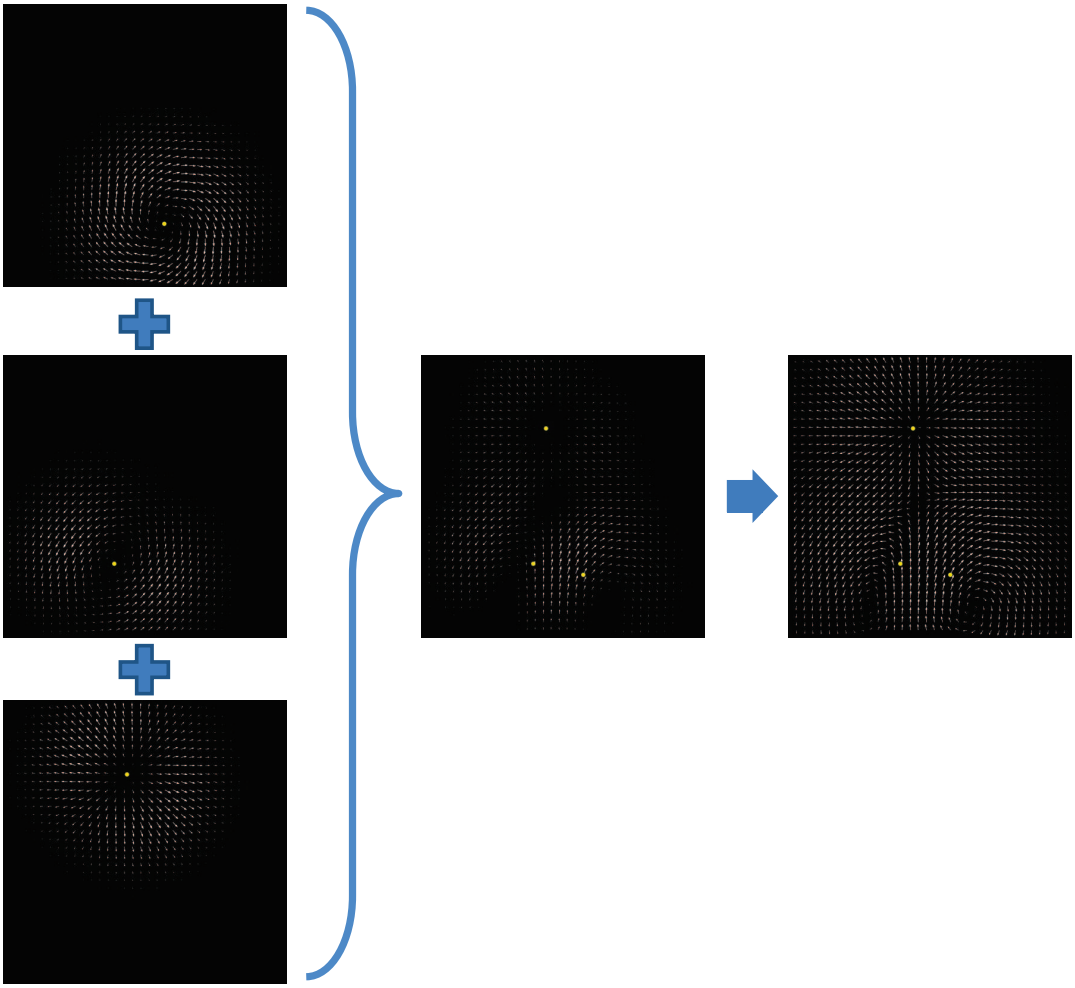

(a) (b) (c)

Figure 1: *Vector field design by composition: (a) randomly placing basis vector fields, each of which contains a single critical point of different types (marked by yellow dots); (b) summation of the basis vector fields in (a); (c) adjusting the magnitude (speed) of the vector field.*

5. Enlarged Images

Figures 4-8 show the enlarged images of Figures 1-5 in the paper.

6. Statistical Analysis Results

Figure 9 lists the detailed results of RM-ANOVA and post hoc test.

References

[FG01] FIRBY P. A., GARDINER C. F.: *Surface topology*, 3 ed. Elsevier, 2001. 1

[JK03] JACOB R. J. K., KARN K. S.: Eye tracking in human-computer interaction and usability research: Ready to deliver the promisess. In *The Mind's Eye: Cognitive and Applied Aspects of Eye Movement Research*, Radach R., Hyona J., Deubel H., (Eds.). Elsevier Science, 2003, pp. 573–603. 1

[PPF*11] POBITZER A., PEIKERT R., FUCHS R., SCHINDLER B., KUHN A., THEISEL H., MATKOVIĆ K., HAUSER H.: The state of the art in topology-based visualization of unsteady flow. *Computer Graphics Forum 30* (2011), 1789–1811. 1

[vW02] VAN WIJK J. J.: Image based flow visualization. *ACM Trans. Graph. 21*, 3 (July 2002), 745–754. 1

[Yar] YARBUS A. L.: *Eye movements and vision*. Plenum Press, New York. 1

[ZMT06] ZHANG E., MISCHAIKOW K., TURK G.: Vector field design on surfaces. *ACM Transactions on Graphics (TOG) 25*, 4 (2006), 1294–1326. 1

© 2015 The Author(s)
Computer Graphics Forum © 2015 The Eurographics Association and John Wiley & Sons Ltd.

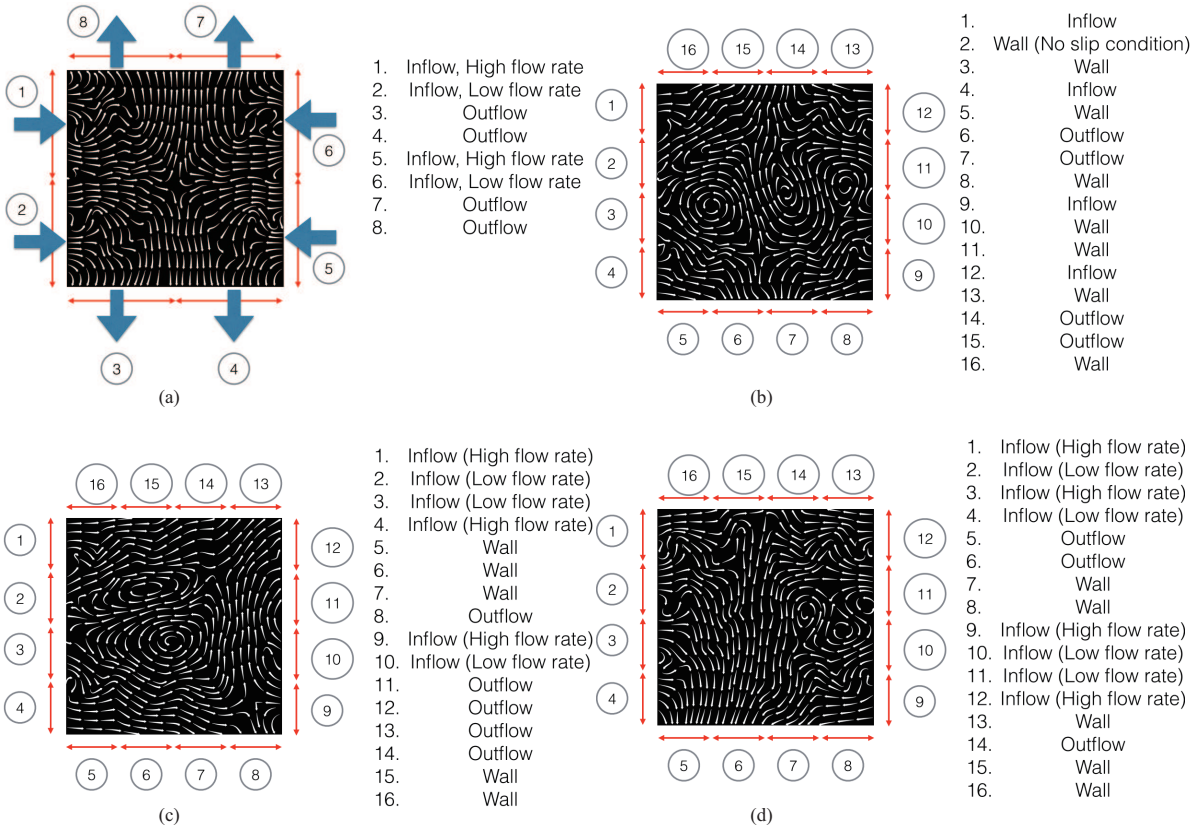

Figure 3: *The four simulated flow fields used in our study and their corresponding boundary conditions.*

© 2015 The Author(s)
Computer Graphics Forum © 2015 The Eurographics Association and John Wiley & Sons Ltd.

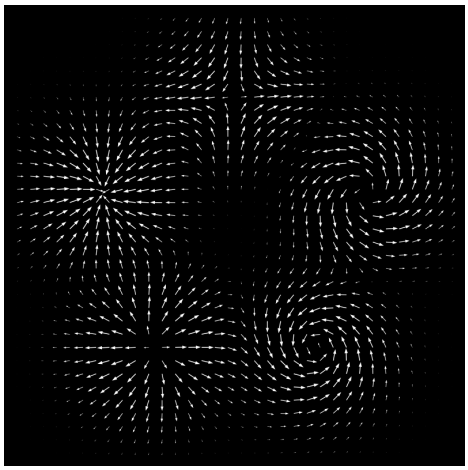

(a) HP

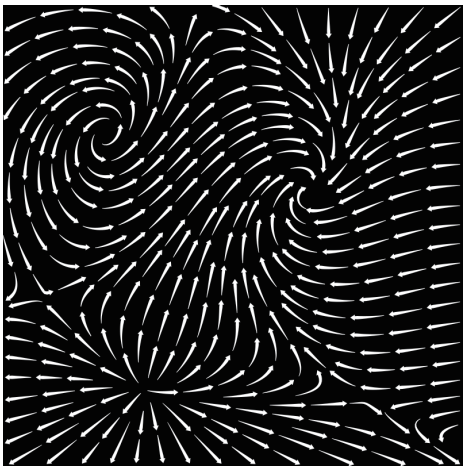

(b) IGS

(c) IS

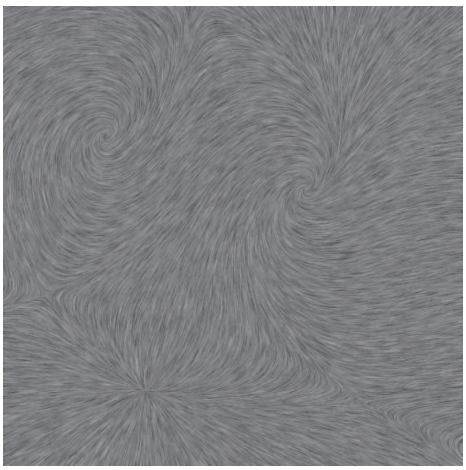

(d) LIC

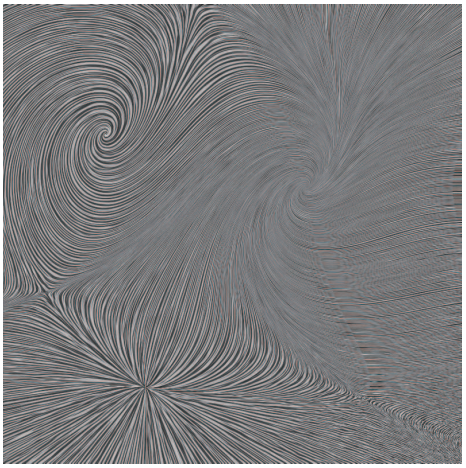

(e) UFLIC

Figure 4: *Examples of five visualization methods evaluated in our user study. (a) Hedgehogs Plot (b) Image-Guided Streamlin (c) Illustrative Streamline (d) Line Integral Convolution (e) is a frame of the animating result generated by Unsteady Flow LIC.*

© 2015 The Author(s)
Computer Graphics Forum © 2015 The Eurographics Association and John Wiley & Sons Ltd.

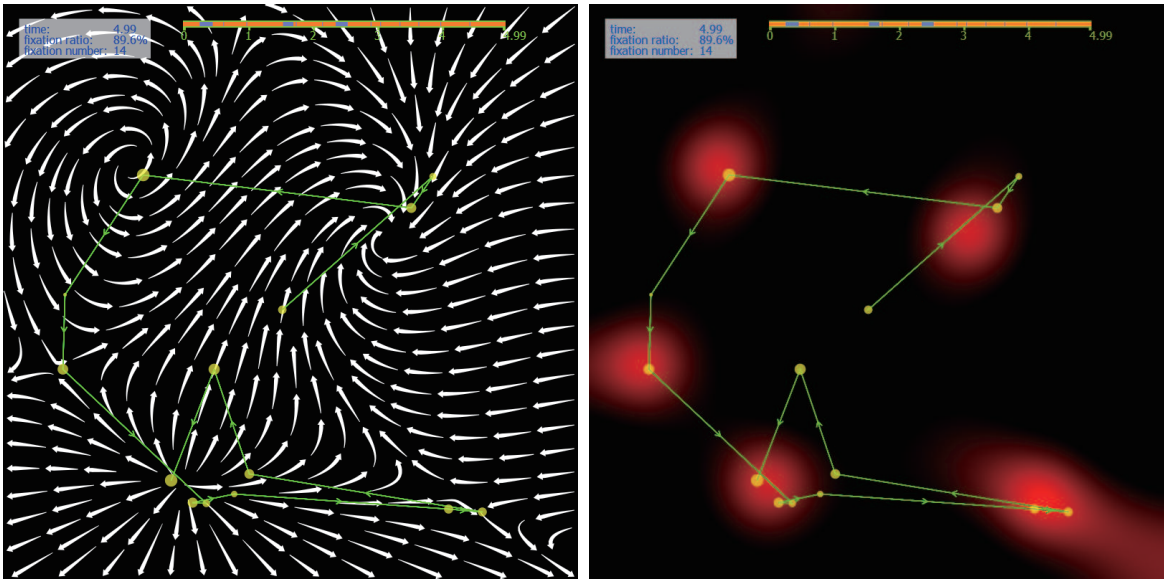

(a) (b)

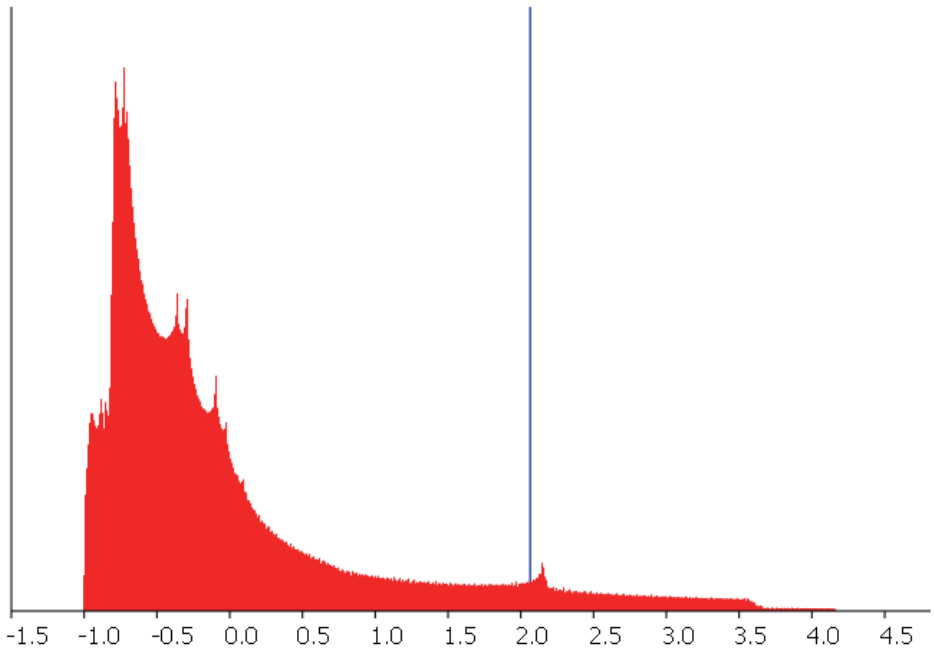

(c)

Figure 5: *An example of NSS score estimation. (a) a participant's eye fixations and scanpath. (b) is a scalar field obtained by computing the directional difference of the flow field, where large values are shown in red color. The orange dots represent eye gaze. (c) is a histogram of (b) normalized by z-score, the blue line shows the weighted mean of entire scanpath.*

© 2015 The Author(s)
Computer Graphics Forum © 2015 The Eurographics Association and John Wiley & Sons Ltd.

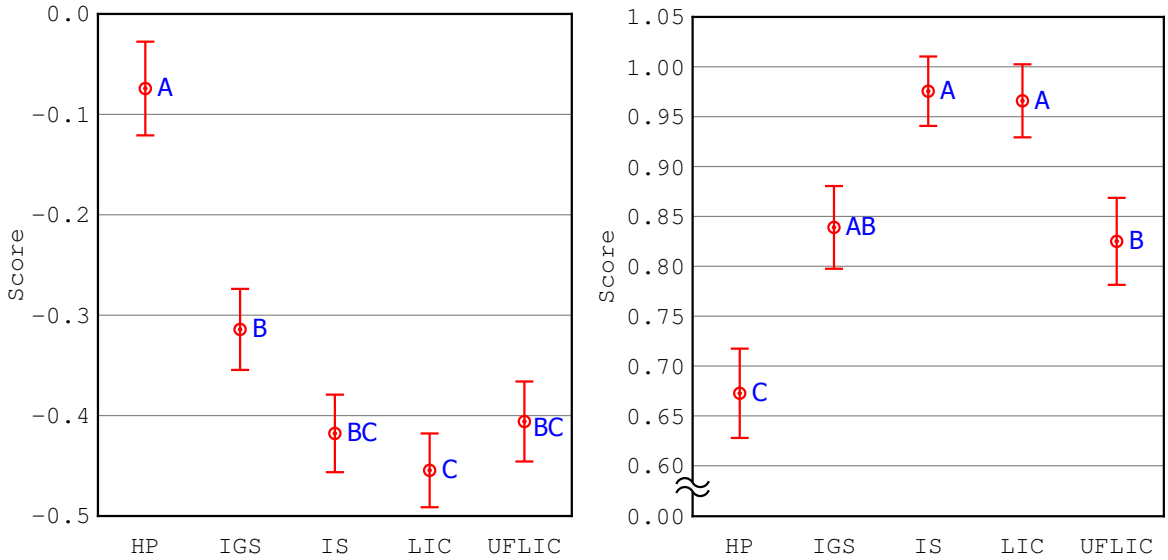

(a) Speed map (b) Distance map

Figure 6: *NSS scores in Exp 1. (a) F(4,659) = 18.52, p < 1e-4. (b) F(4,659) = 11.55, p < 1e-4. The error bars show the standard errors.*

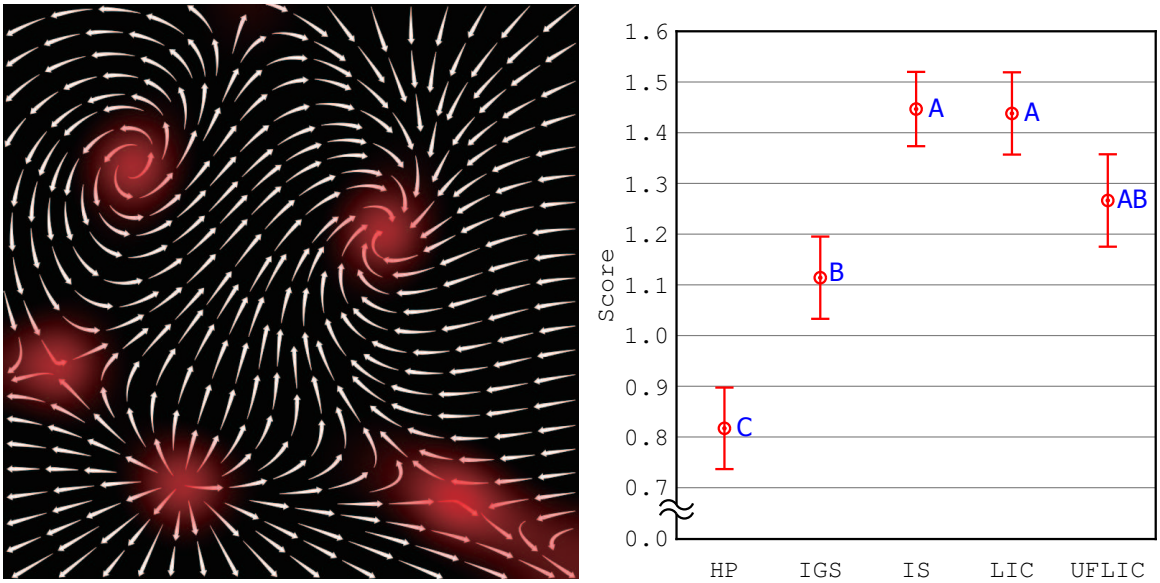

(a) Directional diff. map (b) NSS score

Figure 7: *(a) An example of directional difference map. Red color represents larger directional differences. (b) The NSS scores of directional difference map, F(4,659)= 12.67, p < 1e-4.*

© 2015 The Author(s)
Computer Graphics Forum © 2015 The Eurographics Association and John Wiley & Sons Ltd.

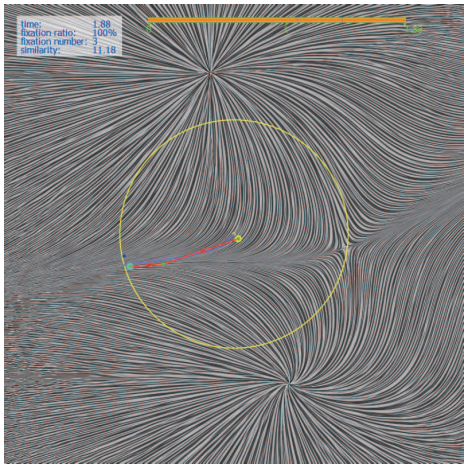

(a) diff.= 11.18

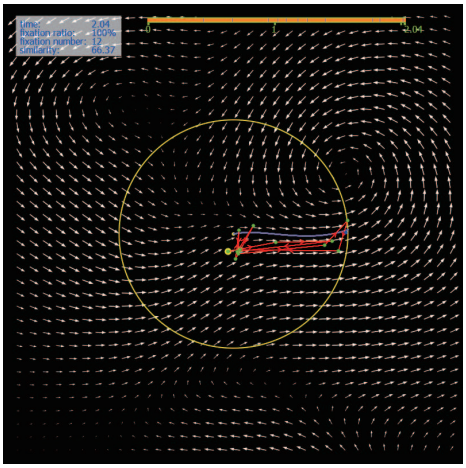

(b) diff.= 66.37

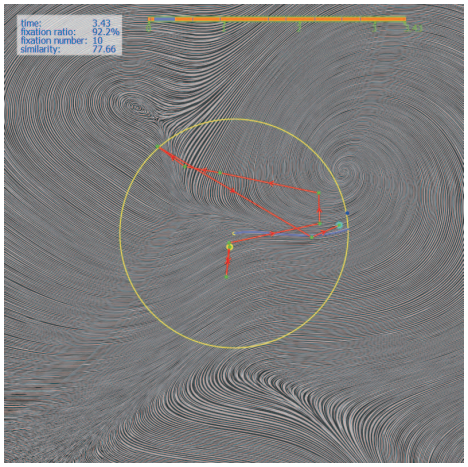

(c) diff.= 77.66

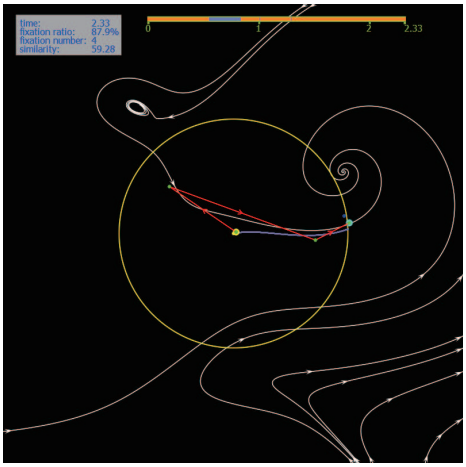

(d) diff.= 59.77

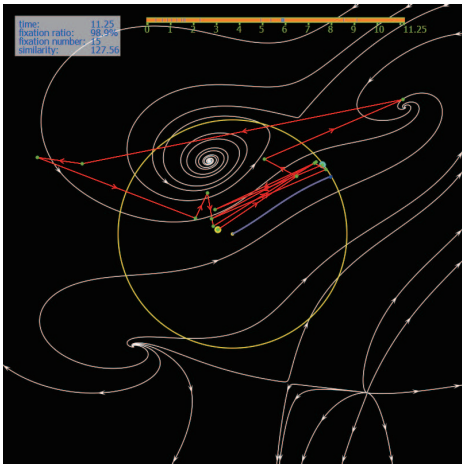

(e) diff.= 127.56

Figure 8: *Five eye scanpathes and their trajectory difference with the pathline in Exp 2. (a) Eye gaze moved with the pathline. (b) Eye gaze kept scanning on the pathline repeatedly. (c) Participant's eye gaze moved to a distant location. (d)(e) Participant focused on arrows first and traced the pathline later.*

© 2015 The Author(s)
Computer Graphics Forum © 2015 The Eurographics Association and John Wiley & Sons Ltd.

Experiment	Variable	Main Effect Result	Comparison Group	Post hoc result
Exp 1	Speed Map	$F(4,659) = 18.52$, $p < .0001$, $R^2 = 0.3$	HP vs. IGS	$F = 22.5418$, ***$p < .0001$
			HP vs. UFLIC	$F = 43.0722$, ***$p < .0001$
			HP vs. IS	$F = 46.2157$, ***$p < .0001$
			HP vs. LIC	$F = 56.6428$, ***$p < .0001$
			IGS vs. LIC	$F = 7.719$, **$p = 0.0056$
	Distance Map	$F(4,659) = 11.55$, $p < .0001$, $R^2 = 0.1$	IS vs. UFLIC	$F = 8.5482$, **$p = 0.0036$
			IS vs. HP	$F = 34.6047$, ***$p < .0001$
			LIC vs. UFLIC	$F = 7.4889$, **$p = 0.0064$
			LIC vs. HP	$F = 32.438$, ***$p < .0001$
			HP vs. UFLIC	$F = 8.7548$, **$p = 0.0032$
			IGS vs. HP	$F = 10.4371$, **$p = 0.0013$
	Directional Difference Map	$F(4,659) = 12.67$, $p < .0001$, $R^2 = 0.3$	HP vs. IS	$F = 36.5728$, ***$p < .0001$
			HP vs. LIC	$F = 35.5711$, ***$p < .0001$
			HP vs. UFLIC	$F = 18.6234$, ***$p < .0001$
			HP vs. IGS	$F = 8.1402$, **$p = 0.0045$
			LIC vs. IGS	$F = 9.6786$, **$p = 0.0019$
			IS vs. IGS	$F = 10.2044$, **$p = 0.0015$
Exp 2	Response Time	$F(2.6,338.2) = 12.2$, $p < .0001$, $R^2 = 0.6$	IS vs. UFLIC	$F = 9.2376$, **$p = 0.0025$
			IS vs. IGS	$F = 26.7319$, ***$p < .0001$
			HP vs. UFLIC	$F = 7.8484$, **$p = 0.0053$
			HP vs. IGS	$F = 24.329$, ***$p < .0001$
	Prediction error	$F(2,265) = 2$, $p = 0.15$, $R^2 = 0.1$		
	Trajectory Difference	$F(2.7,346.1) = 29.03$, $p < .0001$, $R^2 = 0.5$	IS vs. UFLIC	$F = 38.7239$, ***$p < .0001$
			HP vs. IS	$F = 53.5619$, ***$p < .0001$
			IS vs. IGS	$F = 71.9897$, ***$p < .0001$
Exp 3	Response Time	$F(3.4,360.5) = 5.80$, $p = 0.0004$, $R^2 = 0.5$	HP vs. IGS	$F = 8.5842$, **$p = 0.0035$
			HP vs. LIC	$F = 8.7666$, **$p = 0.0032$
			HP vs. UFLIC	$F = 17.1819$, ***$p < .0001$
	Correct Rate	$F(2.6046,273.48) = 10.9$ $p < .0001$, $R^2 = 0.2$	LIC vs. IGS	$F = 14.2635$, **$p = 0.0002$
			LIC vs. IS	$F = 21.7655$, ***$p < .0001$
			HP vs. LIC	$F = 41.5074$, ***$p < .0001$
			IGS vs. UFLIC	$F = 9.6735$, **$p = 0.002$
			IS vs. UFLIC	$F = 15.991$, ***$p < .0001$
			HP vs. UFLIC	$F = 33.3639$, ***$p < .0001$
	Location Error	$F(3.2,339.7) = 66.66$, $p < .0001$, $R^2 = 0.5$	IGS vs. IS	$F = 133.3176$, ***$p < .0001$
			IGS vs. UFLIC	$F = 133.7925$, ***$p < .0001$
			IGS vs. LIC	$F = 144.0364$, ***$p < .0001$
			HP vs. IS	$F = 82.0115$, ***$p < .0001$
			HP vs. LIC	$F = 82.3841$, ***$p < .0001$
			HP vs. UFLIC	$F = 90.4631$, ***$p < .0001$
	Avrage Gaze Distance	$F(3.3,347.8) = 12.71$, $p < .0001$, $R^2 = 0.1$	LIC vs. IS	$F = 13.1697$, **$p = 0.0003$
			IS vs. UFLIC	$F = 9.9737$, **$p = 0.0017$
Exp 4	Response Time	$F(2.5,1090.1) = 60.94$, $p < .0001$, $R^2 = 0.3$	IS vs. HP	$F = 56.9958$, ***$p < .0001$
			IS vs. UFLIC	$F = 120.2547$, ***$p < .0001$
			IS vs. IGS	$F = 129.8974$, ***$p < .0001$
			HP vs. UFLIC	$F = 11.6726$, **$p = 0.0006$
			HP vs. IGS	$F = 14.8048$, **$p = 0.0001$
	Percentage of the First Critical Point Visit is Correct	$F(3,1689) = 1.005$, $p = 0.3896$, $R^2 = 0.004$		
	First-notice Visitis (Green)	$F(2.9,1216.9) = 4.76$, $p = 0.0029$, $R^2 = 0.007$	HP vs. IGS	$F = 10.5322$, **$p = 0.0012$
	Total Visitis (Red)	$F(2.8,1184.6) = 17.59$, $p < .0001$, $R^2 = 0.1$	IS vs. UFLIC	$F = 19.4993$, ***$p < .0001$
			IS vs. IGS	$F = 34.468$, ***$p < .0001$
			HP vs. UFLIC	$F = 12.4863$, **$p = 0.0004$
			HP vs. IGS	$F = 24.8993$, ***$p < .0001$

Figure 9: *RM-ANOVA and post hoc test results.*

© 2015 The Author(s)
Computer Graphics Forum © 2015 The Eurographics Association and John Wiley & Sons Ltd.